Environmental Science and Pollution Research
https://doi.org/10.1007/s11356-022-21506-1

ENVIRONMENTAL TOXICOLOGY: IMPACT ON HUMAN HEALTH

CO_2 gas sensing properties of Na_3BiO_4-Bi_2O_3 mixed oxide nanostructures

Sandeep Gupta[1] · **Anoop Mampazhasseri Divakaran**[2,3] · **Kamlendra Awasthi**[3] · **Manoj Kumar**[3]

Received: 7 January 2022 / Accepted: 12 June 2022

Abstract
In this paper, we report Na3BiO4-Bi2O3 mixed oxide nanoplates for carbon dioxide gas sensing applications. These nanoplates have been synthesized using electrochemical deposition with potentiostatic mode on ITO substrate and characterized using scanning electron microscopy (SEM) and X-ray diffraction (XRD) to analyze their surface morphology and structure. SEM study shows the presence of horizontally aligned nanoplates stacked on top of one another (thickness ≈ 40 to 75 nm). XRD pattern shows the presence of monoclinic Na3BiO4 and Bi2O3. The gas percentage response is evaluated by measuring the change in electrical resistance of the nanoplates in the presence of carbon dioxide for different pressures at 50 °C, 75 °C, and 100 °C. Percentage response of more than 100% is seen at 30 psi gas pressure which increases to ≈ 277% at 90 psi at 100°C.

Keywords Carbon dioxide sensing · Nanostructured bismuth hexagons · Potentiostatic electrodeposition · Nanoplates

Introduction

Modern industrialized society possesses a great threat to our safety and well-being, mainly due to the release of greenhouse gases like carbon dioxide. These gases are responsible for the unstable environmental phenomena like droughts and famines Dimitriou et al. (2021); Shahbazi et al. (2021).

A lot of environmental friendly compounds are being explored for their possible application in solid-state gas sensors. Metal oxide semiconductors and carbon nanotube-based composites are few examples of materials that show good potential for sensing Barsan et al. (2007); Rai et al. (2014); Philip et al. (2003); Rai et al. (2015). Low cost, high sensitivity, and quick response time makes the sensors based on metal oxide semiconductors very attractive. They mainly work by adsorption and desorption of gas on the surface causing a change in their electrical resistance Fine et al. (2010); Seiyama et al. (1962).

Metal oxide sensors based on Bi_2O_3, SnO_2, ZnO, La_2O_3, and Ag-doped CuO have been explored in the past. They tend to give acceptable results at low gas concentrations, but their resistance change at higher concentrations of CO_2 is negligible Shinde et al. (2020). However, nanoplates of Bi_2O_3 showed significant sensing performance even at high concentrations of CO_2 Shinde et al. (2020). This suggests that nanostructures show better sensing characteristics as compared to traditional bulk materials. This may be because a large surface area is highly desirable for a good sensor. Nanostructures provide an ideal way of achieving this, and their morphology has a direct impact on the gas sensing behavior of the material Gurlo (2011).

A number of mixed metal oxide nanostructures have also been explored so far for CO_2 sensing. CuO–$Cu_xFe_{3x}O$ nanocomposite has shown a high response of 50% for CO_2 concentration of 5000 ppm Chapelle et al. (2010). $BaTiO_3$–CuO sputtered thin film has also been used for CO_2 sensing. Resistance change on CO_2 exposure were mainly found to

Responsible Editor: Tito Roberto Cadaval Jr

✉ Sandeep Gupta
sandeep.gupta@ruj-bsdu.in

✉ Manoj Kumar
mkumar.phy@mnit.ac.inn

[1] School of Computing Skills, Bhartiya Skill Development University, Mahindra World City, Jaipur 302037, Rajasthan, India

[2] Department of Physics, Faculty of Science and Technology, Tokyo University of Science, 2641 Yamazaki, Chiba 278-8510 Noda, Japan

[3] Department of Physics, Malaviya National Institute of Technology, JLN Marg, Rajasthan 302017 Jaipur, India

Published online: 21 June 2022

depend on the work function changes in the p-n hetero junctions Herrán et al. (2008); Chavali and Nikolova (2019). Bismuth oxide and its derivatives are also known to show good sensitivity towards CO_2 and other gases Bhande et al. (2011); Gou et al. (2009); Cabot et al. (2004). These compounds are environmental friendly and economical as well.

In this paper, horizontally aligned nanoplates of Na_3BiO_4-Bi_2O_3 mixed oxide have been synthesized using potentiostatic electrodeposition, and their CO_2 sensing properties have been studied at different pressures.

Materials and methods

Materials

Bismuth nitrate pentahydrate ($Bi(NO_3)_3.5H_2O$) used in the current study was purchased from Loba. Sodium nitrate ($NaNO_3$) and nitric acid (HNO_3) were purchased from Merck and Qualigens, respectively.

Synthesis

Potentiostatic electrodeposition with standard three electrode system was used for synthesis with indium tin oxide (ITO)-coated glass plate as working electrode Jiang et al. (2017); Rivera et al. (2017). Platinum wire was used as the auxiliary electrode, and Ag/AgCl (saturated KCl) was used as the reference electrode. Electrolyte was prepared by dissolving bismuth nitrate pentahydrate ($Bi(NO_3)_3.5H_2O$), sodium nitrate ($NaNO_3$), and 69% nitric acid (HNO_3) in distilled water to obtain molarities of 0.013 M, 0.013 M, and 1 M respectively. For horizontally aligned nanoplates, deposition was done at a reduction potential of −0.07 V, 100 rpm stirring speed, and 10-min deposition time. These parameters have been optimized to obtain the desired morphologies Morales et al. (2005).

Sensor setup

A chemiresistor-type sensor has been prepared for studying the gas sensing behavior of these nanoplates (Figure 1). The nanoplates are deposited on to the ITO substrate using potentiostatic electrodeposition. After drying at room temperature, two leads of copper wire were attached using silver paste. This sensor was then installed inside a homemade stainless steel gas sensing chamber (Figure 2). Keithley SourceMeter (2601B) was connected to the sample for resistance measurement at a constant current of 10 mA. Keithley power supply (2600B-250-4 360W) and a Keithley digital multimeter (2700) were used to power the heater and measure the temperature inside the chamber. Inlet and outlet valves were installed to inject and release the gas from the chamber. Chamber pressure was measured with the help of pressure meter fitted at the top of the chamber. CO_2 gas was introduced from a pressurized cylinder (100 % CO_2).

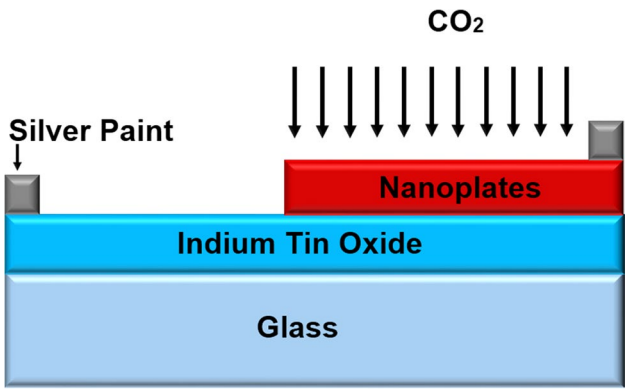

Fig. 1 Schematic device structure of the sensor

Results and discussion

Voltammetric Studies

Figure 3 shows cyclic voltammetry studies on ITO electrode in an electrolyte containing 0.013 M Bi^{3+} ions, 0.013 M Na^+ ions, and 1 M H^+ ions. Peaks corresponding to reduction of cations are seen at cathodic potentials. Similar results have been reported earlier on fluorine-doped tin oxide gas substrate Sadale and Patil (2004). A shift in reduction peak potential is seen in successive cycles. This effect is mainly due to change in the concentrations of reactants and products near the electrode in each cycle Fried (2012).

Morphological studies

SEM image shows the presence of horizontally aligned nanoplates with thickness ranging from 40 to 75 nm (Figure 4). Edge length varies from 4 to 12 μm. These nanoplates appear to be stacked on top of one another with smooth surfaces.

Structural studies

X-ray diffraction pattern shows that the prepared sample is polycrystalline in nature (Figure 5). Major diffraction peaks correspond to Na_3BiO_4 (JCPDS 01-071-1583) and Bi_2O_3 (JCPDS 00-041-1449). Both the oxide phases Na_3BiO_4 and Bi_2O_3 exhibit monoclinic structure. Semiquantitative concentration analysis (PANalytical X'Pert HighScore) shows that the relative fraction of Na_3BiO_4 and Bi_2O_3 phases are 20 % and 80 %, respectively.

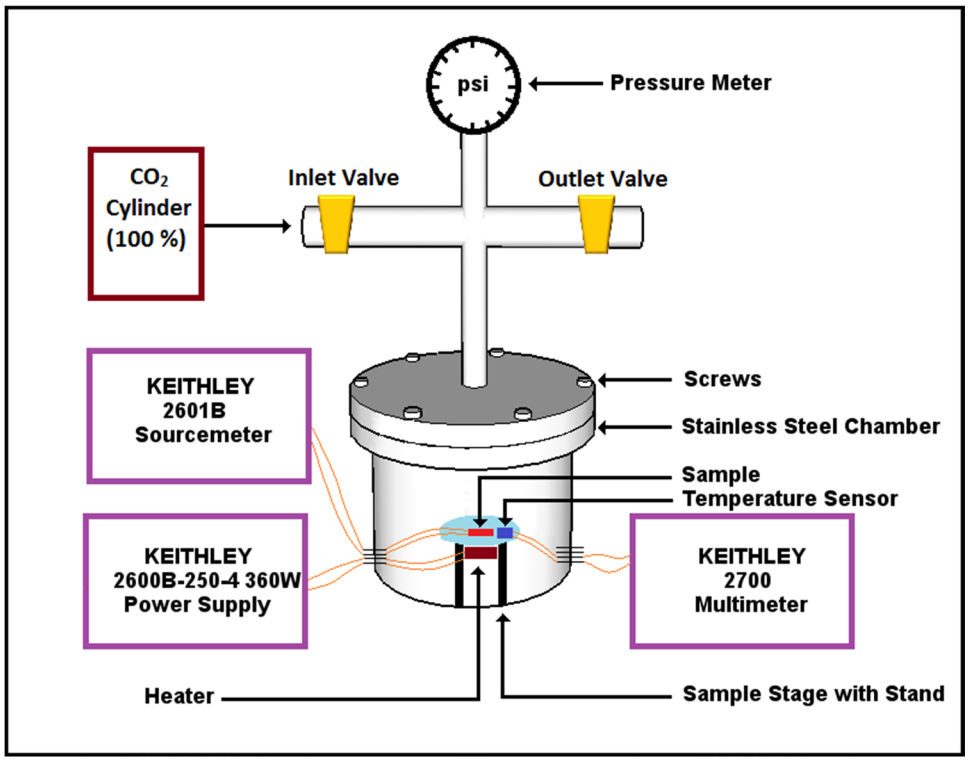

Fig. 2 Schematic diagram of gas sensing setup

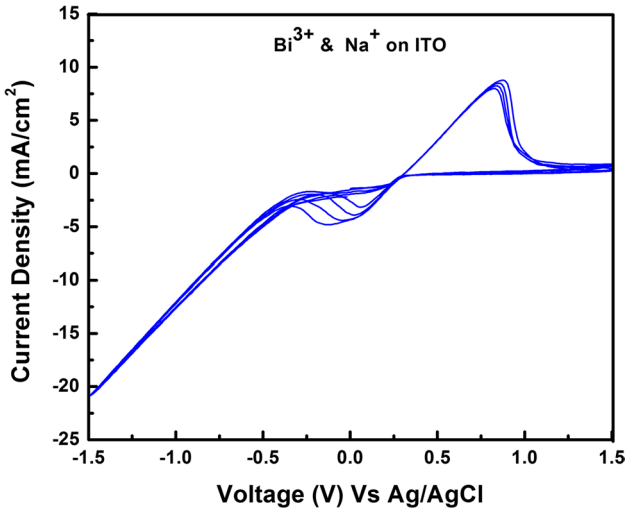

Fig. 3 Cyclic voltammetry curves on ITO in presence Bi^{3+} (0.013 M), Na^{+} (0.013 M), and $H.^{+}$ (1 M)

Gas sensing

The percentage response of the Na_3BiO_4-Bi_2O_3 mixed oxide nanoplates towards CO_2 was determined by measuring the change in resistance of the sample on exposure to carbon dioxide using the formula: Response (%) = $((R_o\text{-}R_g)/R_g)$*100 Rella et al. (1997). R_o is the resistance of sample in presence of air, while R_g is the resistance in presence of CO_2 gas. These measurements were initially carried out at 90 psi CO_2 pressure for 50°C, 75°C, and 100°C (Figure 6). At first, CO_2 gas was flushed trough the chamber to remove the air present in the chamber. The output valve was then closed, and the required CO_2 pressure was built up (indicated by CO_2 ON). In the third step (indicated by CO_2 OFF), inlet valve was closed, and the outlet valve was opened to release the CO_2 pressure. Percentage response of 0%, 15.5%, and 276.8 % was seen at 50°C, 75°C, and 100°C, respectively.

Effect of variation in CO_2 pressure was further evaluated at different pressures and at a fixed temperature of 100°C. Figure 7a, b, and c show the percentage response curve for 90 psi, 60 psi, and 30 psi CO_2 pressures respectively at 100°C. Comparison of response time at different pressures is shown in Figure 8. Details of percentage response, response time, and recovery time are shown in Table 1.

The highest percentage response value of 276.8 % is obtained at 90 psi, which decreases to 254.5 % and 116.5 % at 60 psi and 30 psi, respectively, for Na_3BiO_4-Bi_2O_3 mixed oxide nanoplates. Response time increases (250 ms at 90 psi, 500 ms at 60 psi, and 650 ms at 30 psi), while recovery time decreases (78 s at 90 psi, 53.5 s at 60 psi, and 24.5 s at 30 psi) as the pressure is decreased from 90 to 30 psi This may be due to deeper adsorption of gas molecules at higher pressures. Bi_2O_3 nanoplates prepared by the similar route do not show significant percentage response (3.5 % at 100°C and 90 psi gas pressure), while ITO substrate shows no sensitivity at all. To

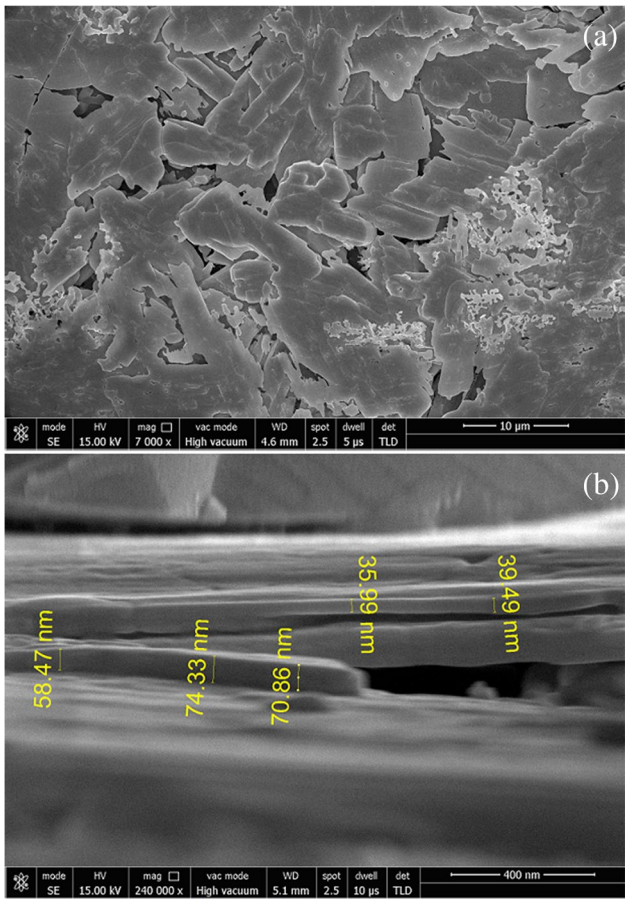

Fig. 4 Scanning electron microscopy images for Na_3BiO_4-Bi_2O_3 mixed oxide nanoplates: **a** top view and **b** cross-sectional view

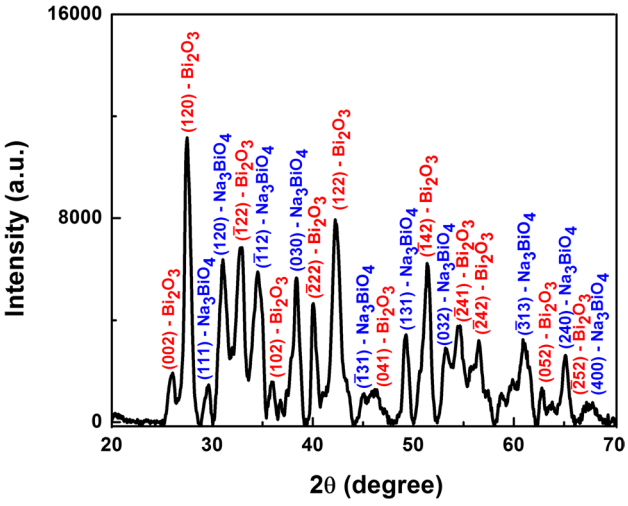

Fig. 5 X-ray diffraction pattern for Na_3BiO_4—Bi_2O_3 mixed oxide nanoplates

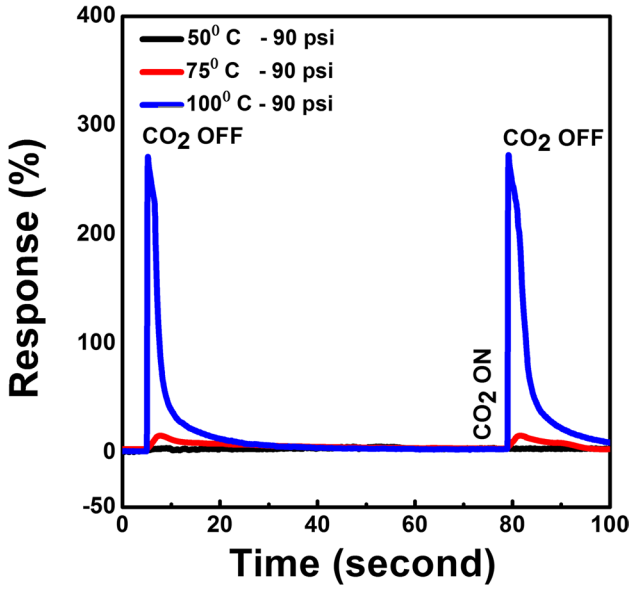

Fig. 6 Percentage response at 90 psi CO_2 pressure at (50° C, 75 °C, and 100 °C) for Na_3BiO_4-Bi_2O_3 mixed oxide nanoplates

further analyze the relationship between CO_2 pressure and percentage response, a linear fit is plotted (Figure 9). A sensitivity of 3.2 %/psi is seen ($R^2 = 0.94$).

Repeatability studies are shown in Figure 10 for 90 psi pressure. Each successive cycle shows similar characteristics with almost equal values for percentage response, response time, and recovery time.

Gas sensing mechanism

The gas sensing mechanism can be explained by taking into account the interaction of CO_2 with the surface nanoplates (Figure 11). An almost instantaneous decrease in resistance is seen on exposure to CO_2 gas.

When the heated metal oxide nanoplates are exposed to air, oxygen gets adsorbed on the surface. At temperatures < 150°C, oxygen is predominantly adsorbed as O^{2-} Ranwa et al. (2014). The detailed mechanism can be explained with the help of following equations:

$$O_2(\text{air}) \rightarrow O_2(\text{adsorbed}) \quad (1)$$

$$O_2(\text{adsorbed}) + 4e^- \rightarrow 2O^{2-} \quad (2)$$

In this process, oxygen takes up electrons from the conduction band. This leads to the formation of an electron depletion layer for an *n*-type material or a hole accumulation layer for a *p*-type material. When an oxidizing gas like CO_2 gas is introduced into an *n*-type metal oxide semiconductor surface, the gas molecules get adsorbed onto the surface of

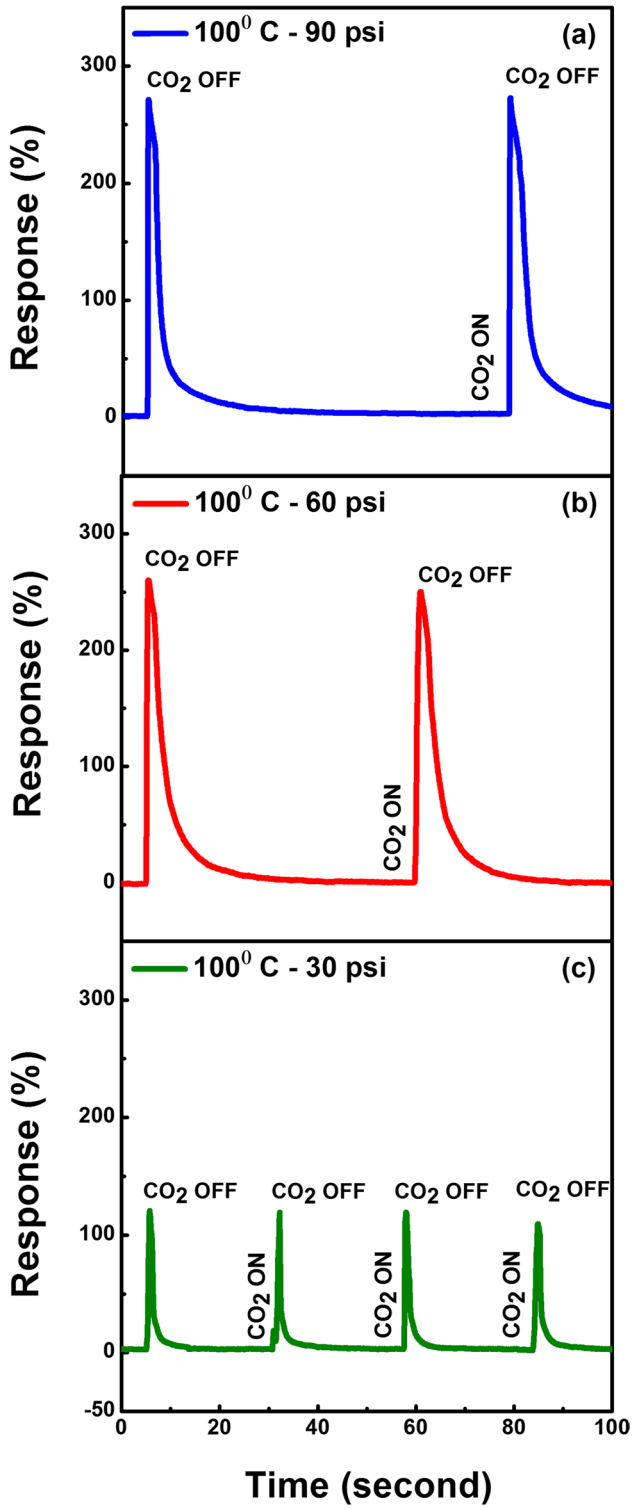

Fig. 7 Percentage response curves for Na_3BiO_4-Bi_2O_3 mixed oxide nanoplates

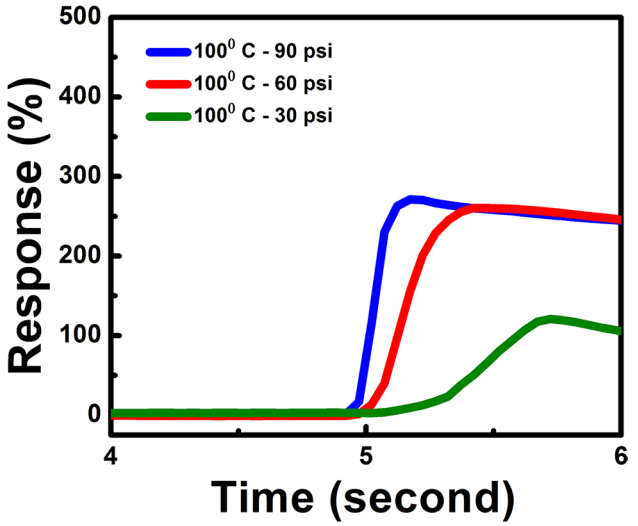

Fig. 8 Comparison of response time at different pressures for Na_3BiO_4-Bi_2O_3 mixed oxide nanoplates

Table 1 Percentage response, response time, and recovery time at 90 psi, 60 psi, and 30 psi CO_2 pressure (100 °C) for Na_3BiO_4-Bi_2O_3 mixed oxide nanoplates

Pressure (psi)	Response (%)	Response time (ms)	Recovery time (s)
90	276.8	250	78.0
60	254.5	500	53.5
30	116.5	650	24.5

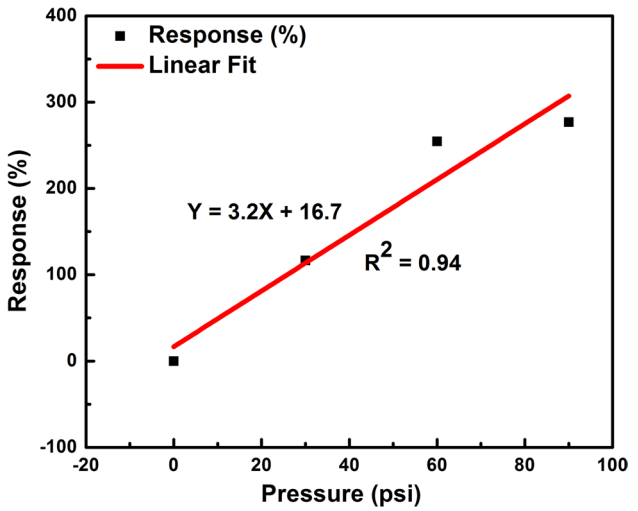

Fig. 9 Linear fit of percentage response for Na_3BiO_4-Bi_2O_3 mixed oxide nanoplates in the range 0 to 90 psi (at 100 °C)

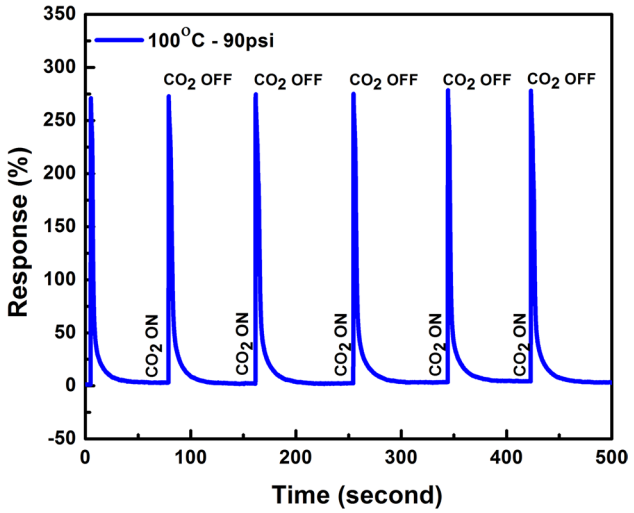

Fig. 10 Percentage response (6 cycles) at 90 psi (100 °C) for Na_3BiO_4-Bi_2O_3 mixed oxide nanoplates

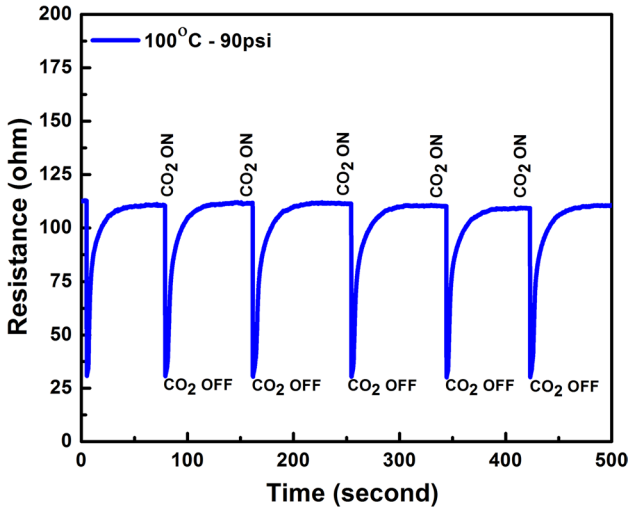

Fig. 11 Resistance change at 90 psi CO_2 pressure and 100 °C for Na_3BiO_4-Bi_2O_3 mixed oxide nanoplates

the material by taking up free electrons. The mechanism of CO_2 adsorption can be understood with the help of the following equations (Bhande et al. (2011)):

$$CO_2 \rightarrow CO + O \tag{3}$$

$$O + 2e^- \rightarrow O^{2-} \tag{4}$$

CO_2 breaks up into CO and O on surface interaction. The oxygen atoms released takes up electrons from the surface forming O^{2-}. This causes a further expansion of electron depletion layer which in turn causes a decrease in conductivity. However, when a *p*-type material is involved, CO_2 causes an

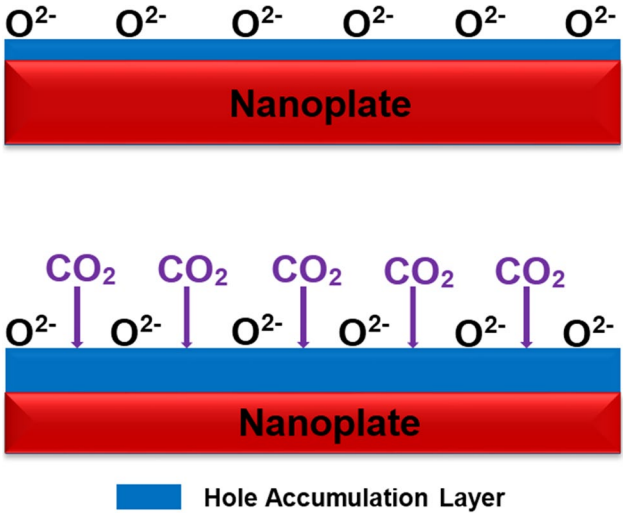

Fig. 12 Schematic diagram of the CO_2 gas sensing mechanism for Na_3BiO_4-Bi_2O_3 mixed oxide nanoplates

expansion of hole accumulation layer thereby causing an increase in conductivity or decrease in resistance Hung et al. (2017).

In the present work, a significant decrease in resistance is observed for Na_3BiO_4-Bi_2O_3 mixed oxide nanoplates on introduction of CO_2 gas (Figure 11). This suggests that this material is behaving as a strong *p*-type semiconductor (Figure 12). Nanoplates offer a very large surface area leading to good adsorption. Results suggest that this adsorption is reversible, and the original conductivity of the material is restored after the gas is removed.

Conclusion

Na_3BiO_4-Bi_2O_3 mixed oxide nanostructures have been synthesized using potentiostatic electrodeposition. XRD analysis shows peaks corresponding to monoclinic Na_3BiO_4 and Bi_2O_3 with weight percentage of 20 % and 80%, respectively. SEM studies reveal the presence of horizontally aligned nanoplates with thickness ranging from 40 to 75 nm. The percentage response shows a linear dependence on pressure in the range of 0 to 90 psi and 100°C ($R^2 = 0.94$). A sensitivity of 3.2 %/psi is observed. These mixed oxide nanoplates shows a very quick response to CO_2 gas, which is a highly sought-after characteristic for a gas sensor. Repeatability and stability makes this material an ideal candidate for sensor development.

Acknowledgements The authors are thankful to the UGC DAE CSR, Indore (CSR-IC/CRS-73/2014/435) for providing financial support. We are also thankful to MRC, MNIT Jaipur for providing characterization facilities.

Author contribution Sandeep Gupta: sample preparation, data acquisition, and writing the draft manuscript.

Anoop Mampazhasseri Divakaran: gas sensing set-up designing and XRD data analysis

Kamlendra Awasthi: supervision of data analysis

Manoj Kumar: conceptualization of research problem and supervision of experiments

Funding This study was financially supported by the UGC DAE CSR, Indore (CSR-IC/CRS- 73/2014/435).

Data availability The authors confirm that the data and materials used in this study are available on request.

Declarations

Ethics approval The authors provide ethical approval for this study.

Consent to participate The authors provide their consent to participate in this study.

Consent for publication The authors provide their consent to publish this study.

Competing interests The authors declare no competing interests.

References

Barsan N, Koziej D, Weimar U (2007) Metal oxide-based gas sensor research: how to? Sens Actuators, B Chem 121(1):18–35

Bhande SS, Mane RS, Ghule AV et al. (2011) A bismuth oxide nanoplate-based carbon dioxide gas sensor. Scripta Mater 65(12):1081–1084

Cabot A, Marsal A, Arbiol J et al. (2004) Bi2o3 as a selective sensing material for no detection. Sens Actuators, B Chem 99(1):74–89

Chapelle A, Oudrhiri-Hassani F, Presmanes L et al. (2010) Co2 sensing properties of semiconducting copper oxide and spinel ferrite nanocomposite thin film. Appl Surf Sci 256(14):4715–4719

Chavali MS, Nikolova MP (2019) Metal oxide nanoparticles and their applications in nanotechnology. SN Applied Sciences 1(6):1–30

Dimitriou K, Bougiatioti A, Ramonet M et al. (2021) Greenhouse gases (co2 and ch4) at an urban background site in Athens, Greece: levels, sources and impact of atmospheric circulation. Atmos Environ 253(118):372

Fine GF, Cavanagh LM, Afonja A et al. (2010) Metal oxide semiconductor gas sensors in environmental monitoring. Sensors 10(6):5469–5502

Fried I (2012) The Chemistry of Electrode Processes. Elsevier Science

Gou X, Li R, Wang G, et al. (2009) Room-temperature solution synthesis of bi2o3 nanowires for gas sensing application. Nanotechnology 20(49):495,501

Gurlo A (2011) Nanosensors: towards morphological control of gas sensing activity. sno2, in2o3, zno and wo3 case studies. Nanoscale 3(1):154–165

Herrán J, Mandayo GG, Castaño E (2008) Solid state gas sensor for fast carbon dioxide detection. Sens Actuators, B Chem 129(2):705–709

Hung CM, Le DTT, Van Hieu N (2017) On-chip growth of semiconductor metal oxide nanowires for gas sensors: a review. Journal of Science: Advanced Materials and Devices

Jiang C, Zeng X, Wu B et al. (2017) Electrochemical co-deposition of reduced graphene oxide-gold nanocomposite on an ito substrate and its application in the detection of dopamine. SCIENCE CHINA Chem 60(1):151–156

Morales J, Sanchez L, Bijani S et al. (2005) Electrodeposition of cu2o: an excellent method for obtaining films of controlled morphology and good performance in li-ion batteries. Electrochem Solid-State Lett 8(3):A159–A162

Philip B, Abraham JK, Chandrasekhar A et al. (2003) Carbon nanotube/PMMA composite thin films for gas-sensing applications. Smart Mater Struct 12(6):935

Rai P, Jeon SH, Lee CH, et al. (2014) Functionalization of ZnO nanorods by CuO nanospikes for gas sensor applications. RSC Advances 4(45):23,604–23,609

Rai P, Majhi SM, Yu YT, et al. (2015) Noble metal@ metal oxide semiconductor core@ shell nano-architectures as a new platform for gas sensor applications. RSC Advances 5(93):76,229–76,248

Ranwa S, Kulriya PK, Sahu VK, et al. (2014) Defect-free ZnO nanorods for low temperature hydrogen sensor applications. Applied Physics Letters 105(21):213,103

Rella R, Serra A, Siciliano P et al. (1997) Co sensing properties of sno2 thin films prepared by the sol-gel process. Thin Solid Films 304(1–2):339–343

Rivera M, Martinez-Vado F, Mendoza-Huizar L, et al. (2017) Morphological and local magnetic properties of cobalt clusters electrodeposited onto indium tin oxide substrates. Journal of Materials Science: Materials in Electronics pp 1–7

Sadale S, Patil P (2004) Nucleation and growth of bismuth thin films onto fluorine-doped tin oxide-coated conducting glass substrates from nitrate solutions. Solid State Ionics 167(3):273–283

Seiyama T, Kato A, Fujiishi K et al. (1962) A new detector for gaseous components using semiconductive thin films. Anal Chem 34(11):1502–1503

Shahbazi H, Abolmaali AM, Alizadeh H et al. (2021) Development of high-resolution emission inventory to study the relative contribution of a local power plant to criteria air pollutants and greenhouse gases. Urban Climate 38(100):897

Shinde PV, Shinde NM, Shaikh SF, et al. (2020) Room-temperature synthesis and CO 2-gas sensitivity of bismuth oxide nanosensors. RSC Advances 10(29):17,217–17,227